

NRL Report 7287

Application of a Scanned-Laser  
Active Imaging System  
to Atmospheric and Underwater  
Viewing Environments

R.W. Waynant

High Temperature Physics Branch  
Plasma Physics Division

August 24, 1971

Approved for public release; distribution  
unlimited

## DOCUMENT CONTROL DATA - R &amp; D

(Security classification of title, body of abstract and indexing annotation must be entered when the overall report is classified)

1. ORIGINATING ACTIVITY (Corporate author) Naval Research Laboratory Washington, D.C. 20390		2a. REPORT SECURITY CLASSIFICATION Unclassified	
		2b. GROUP	
3. REPORT TITLE APPLICATION OF A SCANNED-LASER ACTIVE IMAGING SYSTEM TO ATMOSPHERIC AND UNDERWATER VIEWING ENVIRONMENTS			
4. DESCRIPTIVE NOTES (Type of report and inclusive dates) An interim report on the problem.			
5. AUTHOR(S) (First name, middle initial, last name) Ronald W. Waynant			
6. REPORT DATE August 24, 1971		7a. TOTAL NO. OF PAGES 20	7b. NO. OF REFS 7
8a. CONTRACT OR GRANT NO. NRL Problem N01-24		9a. ORIGINATOR'S REPORT NUMBER(S) NRL Report 7287	
b. PROJECT NO. RR 104-03-41		9b. OTHER REPORT NO(S) (Any other numbers that may be assigned this report)	
c.			
d.			
10. DISTRIBUTION STATEMENT Approved for public release; distribution unlimited.			
11. SUPPLEMENTARY NOTES		12. SPONSORING MILITARY ACTIVITY Department of the Navy Office of Naval Research Arlington, Virginia 22217	
13. ABSTRACT A scanned-laser active imaging system employing a synchronously scanned image-dissector detector was analyzed from the standpoint of how much resolution would be available to an observer viewing a CRT display. Graphical results are given of the system performance in atmospheric and underwater environments as well as of the effects of laser power, wavelength, and the addition of image intensifiers to the receiving system. The novelty of the analysis is that it directly predicts the detection performance of the human observer when aided by a scanned-laser active imaging system. The performance of such a system compares favorably with range-gated active imaging systems.			

14. KEY WORDS	LINK A		LINK B		LINK C	
	ROLE	WT	ROLE	WT	ROLE	WT
Laser Active imaging Scanned laser Image dissector Observer resolution Underwater observations						

## CONTENTS

Abstract	ii
Problem Status	ii
Authorization	ii
NOTATION	1
INTRODUCTION	2
EQUILIBRIUM OF A LOADED CABLE	2
THE EXTENDED METHOD	4
Basic Concepts	4
Iterative Procedure	7
Numerical Example I	8
Irrelevancy of the Location of the Internal Cut	12
GENERALIZATION TO ARBITRARY CABLE ARRAYS	13
General Theory	13
Numerical Example II	16
STATICALLY UNSTABLE CABLE ARRAYS	18
CONFIGURATION-DEPENDENT EXTERNAL FORCES	21
CONCLUSIONS	22
REFERENCES	22
APPENDIX – Proof of the Convergence and the Uniqueness of the Extended Method of Imaginary Reactions	23

## ABSTRACT

A method is presented for determining the tensions in, and equilibrium configuration of, internally redundant structural cable arrays. The method has applications to suspension bridges, structural nets, and moorings. Cable stretch is included in the formulation, and arbitrary strain-tension relations are permitted. An iterative solution, that does not require the calculation of slopes or derivatives, is generated for varying the unknown redundant reactions. Global convergence of the iteration to the correct reactions (and consequently to the correct equilibrium configuration of the array) from any set of initially guessed reactions is insured. The rapidity of this convergence is demonstrated by several numerical examples. Although the basic solution assumes external loads that are independent of the array configuration, a combination of the method with the mathematical technique of successive approximations allows configuration-dependent loadings to also be treated. This combined technique is described.

## PROBLEM STATUS

This is an interim report; work is continuing on other phases of the problem.

## AUTHORIZATION

NRL Problem F02-24  
Project RR 009-03-45-5807

Manuscript submitted April 23, 1971.

THE ANALYSIS OF INTERNALLY REDUNDANT  
STRUCTURAL CABLE ARRAYS

NOTATION

The symbols used in this report are defined below. Occasionally, when no confusion can arise, the subscript  $n$  is suppressed.

$A_n$	the position vector of the anchor point of the $n$ th cable
$a_n, b_n, c_n$	respectively the X, Y, and Z components of $A_n$
$E$	a positive definite error function
$E'$	a trial iterative value of $E$
$F_n$	the vector point forces acting on a cable array
$f_n(s_n)$	the vector load per unit of unstressed length acting on the $n$ th cable
$I_n$	the vector imaginary reactions applied to a cable array
$I'_n$	a trial iterative value of $I_n$
$i, j, k$	respectively the unit vectors along the X, Y, and Z axes
$L_n$	the unstressed length of the $n$ th cable
$P_n(s_n)$	the position vector of a point on the $n$ th cable
$R_n(s_n)$	the resultant force vector at a point on the $n$ th cable
$R_{nX}, R_{nY}, R_{nZ}$	respectively the X, Y, and Z components of $R_n$
$s_n$	the measure of unstressed arc length along the $n$ th cable
$T_n(s_n)$	the tension at a point on the $n$ th cable
$X, Y, Z$	the axes of a Cartesian coordinate system
$x, y, z$	respectively the X, Y, and Z components of $P_n$
$\Delta I_n$	the vector change in $I_n$ ( $I'_n = I_n + \Delta I_n$ )
$\delta$	a positive convergence factor having the dimension of force
$\epsilon_n(s_n)$	the strain at a point on the $n$ th cable
$\xi$	a dummy variable of integration

## INTRODUCTION

In Refs. 1 and 2 the present authors introduced a new technique for determining the equilibrium configuration of complex, externally redundant cable arrays. This technique was termed the Method of Imaginary Reactions. In essence, the method of analysis was an extension of consistent deformation theory to a highly nonlinear problem. That is, the solution consisted of releasing the external redundants and replacing their effects by a set of guessed, or imaginary, reactions. This created a statically determinant cable array for which the equilibrium configuration could be readily calculated. The guessed reactions were then varied until the calculated configuration of the array satisfied the initial geometric constraints on the problem.

The usefulness of the Method of Imaginary Reactions was in the simple iterative technique presented for varying the redundant reactions, the rapid and global convergence of the iteration to the correct reactions from any set of initially guessed reactions, and the adaptability of the technique to the computer.

The only restriction placed on the method was that no internal loops of cable existed in the system. Such loops (for example, ABC in Fig. 1) introduced internal redundancies into the system and prevented the determination of the array configuration even after all external redundants had been released.

In this report the restriction on the Method of Imaginary Reactions to externally redundant arrays is removed, and the method is extended to the analysis of arbitrary, internally redundant cable systems. This technique of solution is termed the "Extended Method of Imaginary Reactions."

Pahuja (3) previously worked on this problem, but his analysis was limited to the array in Fig. 1. Impetus for the present solution has been generated by several internally redundant arrays, considerably more complex than the one studied by Pahuja, recently proposed for naval oceanographic and ASW programs. Prior to this development the response of these moors to their environmental loadings (weight forces, buoyancy forces, and hydrodynamic forces) could only be hypothesized, not predicted; thus the evaluation of their performance was, at best, tenuous.

The Extended Method of Imaginary Reactions preserves both the simplicity and the globally convergent property of the original method. The only limitation placed on the Extended Method is that the cables comprising the array must be perfectly flexible. Within this limitation, arbitrary cable constitutive (strain-tension) relations are allowed. Also, the cable array is assumed to be statically stable; that is, under the action of the applied forces, no cable section has zero tension. However, if zero tension occurs, the method still produces convergence but to a self-consistent equilibrium configuration. This case is discussed, and it is shown that preliminary stability investigations are unnecessary.

## EQUILIBRIUM OF A LOADED CABLE

Prior to the development of the Extended Method of Imaginary Reactions, consider the equilibrium configuration of the loaded cable shown in Fig. 2. In this figure, X, Y, and Z (with corresponding unit vectors  $i$ ,  $j$ , and  $k$ ) represent the axes of a right-handed Cartesian coordinate system. With respect to this system, the location of the cable anchor point is given by the vector  $A$  with components

$$A = a_i + b_j + c_k ,$$

In Eq. (5),  $\lambda$  is the wavelength of the illumination in nanometers, and  $v$  is the visibility in kilometers. The power received by the dissector is

$$P(r) = \frac{Y_1^2 \rho W e^{-2ar}}{2r^2}, \tag{6}$$

where  $\rho$  is the reflectivity of the illuminated area. The reflection has been assumed isotropic over a hemisphere. Knowing the quantum efficiency  $q$  and the number of photons per joule  $K$ , the signal current of the detector can be calculated. Table 1 shows some typical laser powers, the quantum efficiency at each wavelength, the number of photons per joule, and the signal currents.

Table 1  
Power and Associated Characteristics of Currently Available Lasers

Power $W$ (watts)	Wavelength $\lambda$ (Å)	Quantum Efficiency $q$ (%)	$K$ ( $\times 10^{18}$ photons/joule)	Signal Current $i_s$ (mA)
0.1	6328	6	3.19	30.6 $P(r)$
5	5000	14	2.52	56 $P(r)$
200	10600	0.4	5.34	3.42 $P(r)$
1000	10600	0.4	5.34	3.42 $P(r)$

Following Rosell (2), the signal-to-noise ratio (SNR) of the display can be determined. The video SNR can be written as

$$SNR_{video} = \frac{CG_M i_s / E_v E_h}{\left[ \frac{G_m^2 e \Delta f i_s}{E_v E_h} + \sum_{m=1}^M \frac{(G_{Mss}) \left[ \frac{(G_{Mss})^{M-m}}{E_v E_h} \right]^2}{E_v E_h} \right]^{1/2} e \Delta f i_s + I_{pa}^2} \tag{7}$$

where  $G_M$  is the total photomultiplier gain,  $G_{Mss}$  is the gain of a single stage of the photomultiplier,  $C$  is the contrast,  $\Delta f$  is the bandwidth of the system,  $e$  is the electron charge,  $E_v E_h$  is the scan efficiency,  $I_{pa}$  is the preamplifier noise, and  $i_s$  is the signal current. Table 2 gives typical values of these quantities for a specific image-dissector tube.

The video signal must be modified by the modulation transfer function of the image dissector itself. Let  $N$  be the spatial frequency in TV lines per picture height. For the image dissector the transfer function is governed by the aperture itself. For an aperture of 0.0005 in., the transfer function is shown in Fig. 2. With this modification the video SNR is now a function of spatial frequency  $N$ . (Obviously, all transmission and transfer losses have been neglected in the receiver optics. Generally these losses are rather minor.) The display SNR can now be found from the modified video SNR and is given by

$$SNR(N)_{display} = \frac{(0.75t\Delta f)^{1/2}}{N} SNR(N)_{video} \tag{8}$$

where  $t = 0.2$  sec is the integration time of the eye. Presented with such a display, the human brain is now asked whether a particular pattern exists on the display. What is

**Table 2**  
**Characteristics of a System Using**  
**a WX 30029 Image-Dissector Tube**

$G_M = 1.7 \times 10^5$
$G_{Mss} = 2.36$
$M = 14$ stages
$e = 1.6 \times 10^{-19}$ coul
$\Delta f = 5 \times 10^4$ Hz
$E_v E_h = 0.79$ (for TV broadcast)
$I_{pa} = 5 \times 10^{-9}$ A (typical)

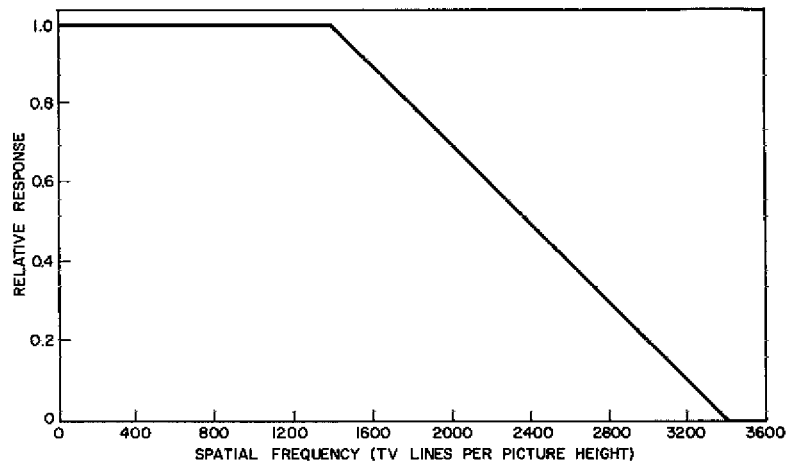


**Fig. 2 - Approximate aperture response of a**  
**WX-30029 image dissector**

needed, in the author's opinion, is a receiver operating curve (ROC) for the human brain. Similar curves are quite common for electrical communication systems, but, to the author's knowledge, there has not been an attempt to obtain an ROC for the eye-brain receiver system. Several determinations have been made which attempt to specify the display SNR required for a 50% probability of detecting simple targets. The ratios vary from about 1 to 10. From past experience in the laboratory, the best number seems to be about 3.25, since it was measured for a variety of square patterns. Recognizing that limitations exist, an SNR of 3.25 can be used as a detection criterion, and the observer performance of the system can be calculated as a function of the system variables. In particular, plots can be made of resolution available (number of TV lines/picture height) vs range to the target with visibility, laser power, and contrast as the variables.

Table 1 lists the characteristics of several of the CW lasers that can be purchased currently along with the signal current per unit of power received from the target. These values have been used to calculate system performance. Figures 3 through 6 show

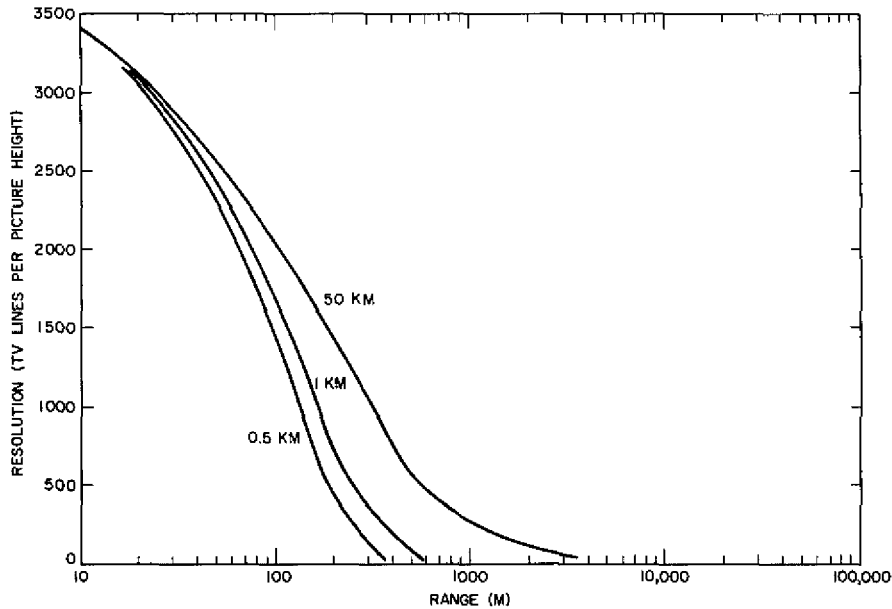


Fig. 3 - Display resolution vs range at 50-km, 1-km, and 0.5-km visibilities for a 0.1-W, 6328-Å laser

the available resolution from each system vs range for various atmospheric visibilities. Figure 7 compares the systems for the case of 50 km (exceptionally good visibility). The two high-power infrared systems suffer from low quantum efficiency at this wavelength.\* A really high power in the visible region, where quantum efficiency is high, would greatly improve the system performance.

In all of the figures presented so far, 100% contrast has been assumed between an object and its background. This contrast rarely occurs in actual viewing situations. Figure 8 shows how a reduction in contrast to 30% or 10% reduces the resolution at any given range for one of the above systems. A reduction in contrast obviously reduces the resolution of the observer significantly.

No attempt has been made to include aperture losses from the receiver optics. This is quite easy once one has selected the optics. Also, after this selection, the spatial resolution predicted for an observer can be converted into a resolution element size at a distance  $r$ . This parameter is of value in estimating the size of the target which can be recognized.

#### Meaning of Resolution to the Observer

Figures 3 through 8 show the resolution available to the observer as a function of the distance from the transmitter/receiver to the object. It may be more meaningful to relate these numbers to the size of the object that can be acquired, recognized, or identified. This is given by

\*Considerable progress has been made in this area recently which should result in improved systems.

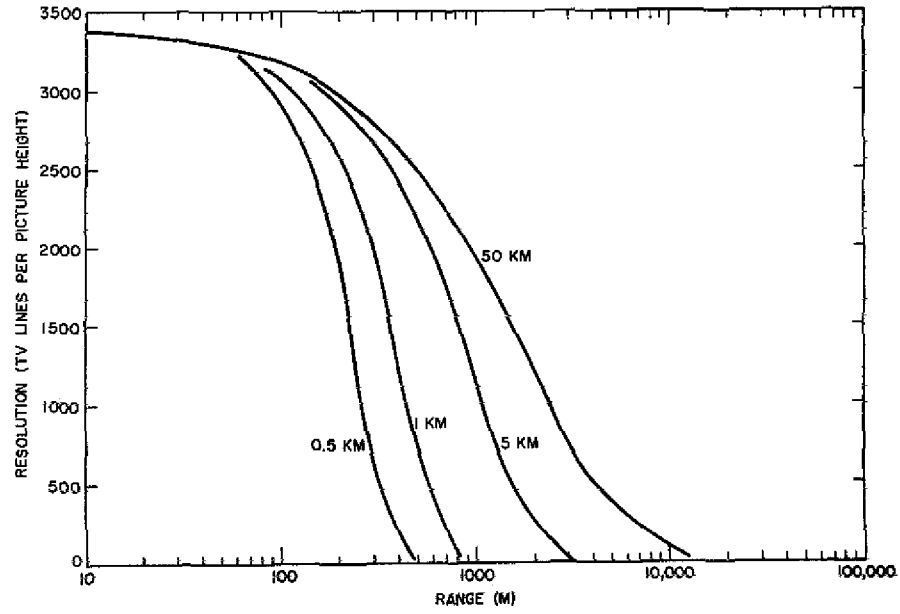


Fig. 4 - Display resolution vs range at 50-km, 5-km, 1-km, and 0.5-km visibilities for a 5-W, 5000-Å laser

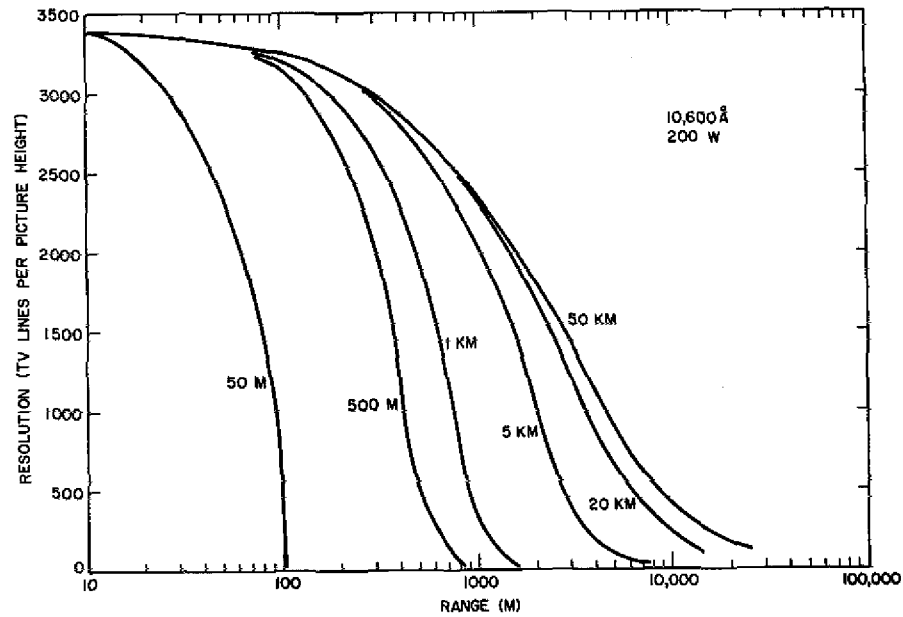


Fig. 5 - Display resolution vs range at 50-km, 20-km, 5-km, 1-km, 0.5-km, and 0.05-km visibilities for a 200-W, 10,600-Å laser

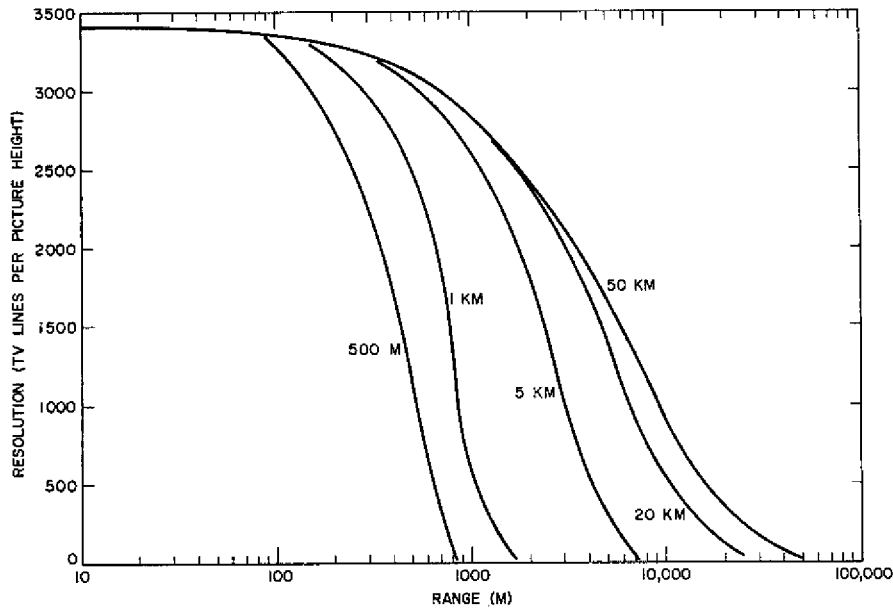


Fig. 6 - Display resolution vs range at 50-km, 20-km, 5-km, 1-km, and 0.5-km visibilities for a 1000-W, 10,600-Å laser

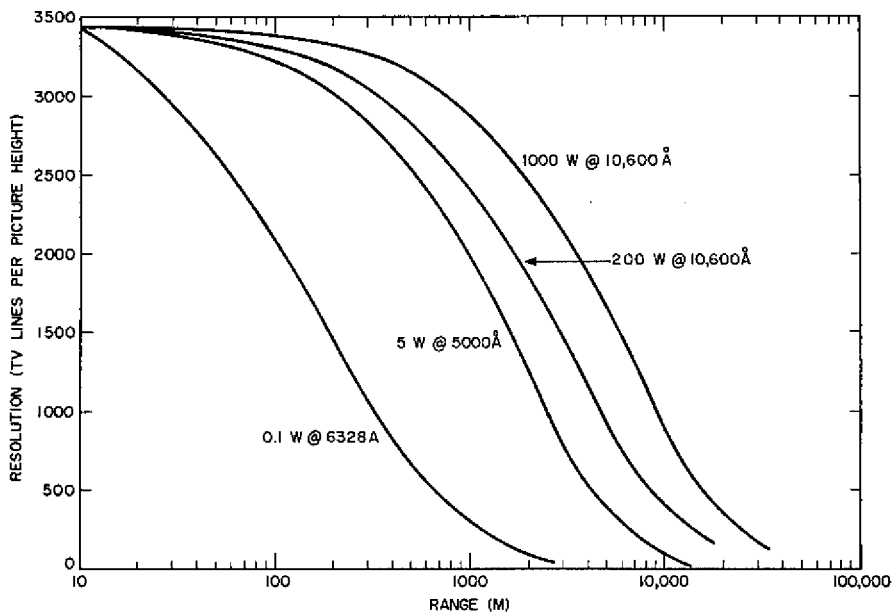


Fig. 7 - Display resolution vs range for the various laser wavelengths and powers at a 50-km visibility

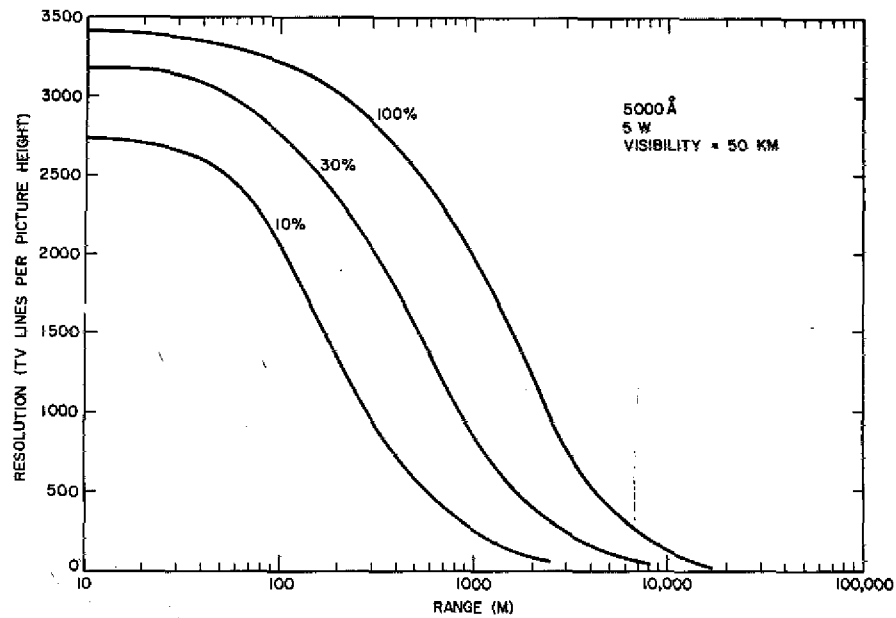


Fig. 8 - Change in display resolution as the contrast drops from 100% (as assumed in all previous figures) to 30% or 10%

$$X = \frac{0.6 D_{pc} R}{N_{TV} F_L} \quad (9)$$

where  $X$  is the object dimension,  $D_{pc}$  is the photocathode diameter,  $R$  is the range,  $N_{TV}$  is the number of resolution elements available, and  $F_L$  is the focal length of the objective lens. It is generally agreed that two to four resolution elements of size  $X$  are required to say that an object has been acquired (something's there), six to eight elements are needed to recognize the object (it's a vehicle), and ten to twelve elements are needed to identify it (it's a car, truck, etc.).

One way of using this information is to assume that identification requires 10 TV lines/picture height and to pick other system parameters of 1 in. for the photocathode diameter and 6 in. for the focal length of the lens. With these parameters, Eq. (9) becomes  $X = 0.1R$ . Using the graphical information, one can find where the resolution  $N_{TV} = 10$  intersects the curve and then the corresponding  $R$  can be found. Knowing  $R$ ,  $X$  can be found and compared with expected object dimensions. At distances shorter than  $R$ , more resolution elements are available, and smaller objects can be identified in the display.

Perhaps a more useful way of using Eq. (9) is, at any range, to divide the available  $N_{TV}$  by the required elements (e.g., ten for identification) and then to calculate  $X$ . For example, in Fig. 7, for 0.1 W at 6328 Å, 2000 TV lines are available at 100 m. Dividing  $N_{TV}$  by ten for identification and using the  $D_{pc}$  and  $F_L$  from above, the smallest element identifiable is 5 cm. At a 1000-m range,  $N_{TV}$  has dropped to about 200, and the smallest element is 5 m.

By applying these calculations to a specific system being designed, the performance of the system in terms of detectable object size can be predicted in advance.

### Addition of Intensifiers to the Image Dissector

The image dissector has been used for many high-resolution pickup tasks. The low sensitivity due to the small aperture has normally restricted the tube to use with sources of relatively high intensity. In this application the small aperture presents no limitation (as long as the laser return is synchronized to fall within the aperture), but any increase of the returning light beam will improve the system performance. Image intensifiers are convenient devices for amplification of the return beam. Several stages can be cascaded to enable the system to perform better in severely attenuating environments.

In general, one can expect a coupling gain of about 40 per stage of image intensifier. In addition, the transfer function of each stage of intensification must be taken into account, and this may be a limiting factor. Adding  $n$  stages of intensification has the effect on the video SNR given in Eq. (7) of changing  $i_s$  to

$$i_s = (40)^n KP(r) . \quad (10)$$

The video signal is modified by the aperture transfer function of both the dissector and the intensifier(s). Figure 9 shows a typical aperture response of an image intensifier. The display SNR can then be calculated by using Eq. (8) and a modification such that

$$\text{SNR}(N)_{\text{video}} + \text{intensifiers} = \text{SNR}(N)_{\text{video}} I^n D^n(N) , \quad (11)$$

where  $I$  is the gain of the intensifier (40 is assumed in this analysis) and  $D(N)$  is the aperture response of an intensifier as shown in Fig. 9.

System results for one and two stages of intensification are given in the Figs. 10 through 15 for vision in the atmosphere. Short-range resolution suffers greatly because of the aperture response of the intensifier(s). Long-range resolution is greatly improved because of the increased illumination presented to the dissector.

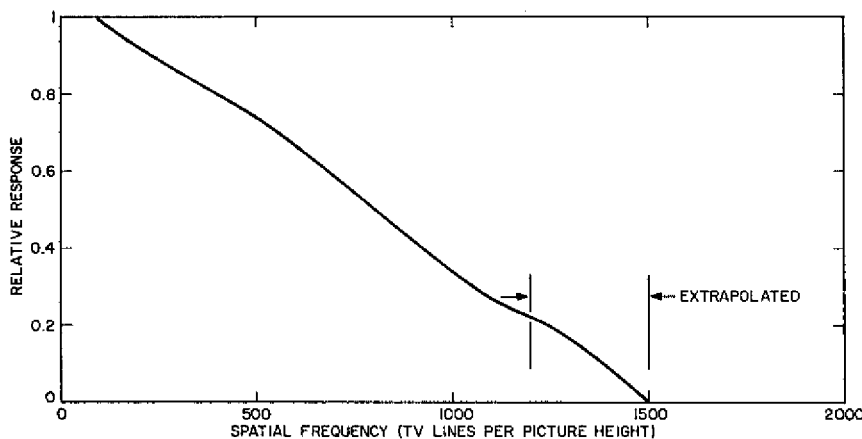


Fig. 9 - Aperture response of a 25-mm image intensifier

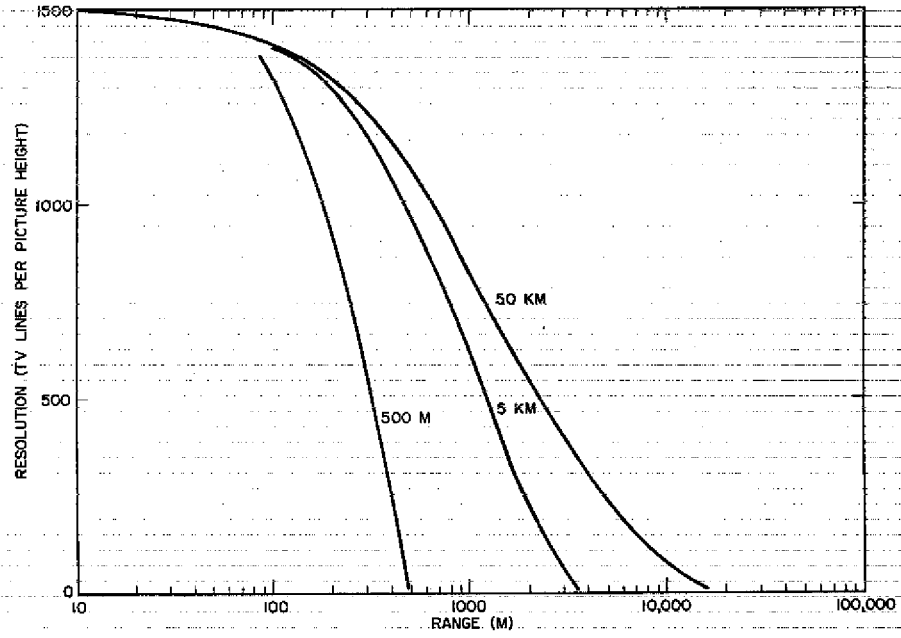


Fig. 10 - Display resolution vs range for the system of Fig. 3 with one image intensifier added

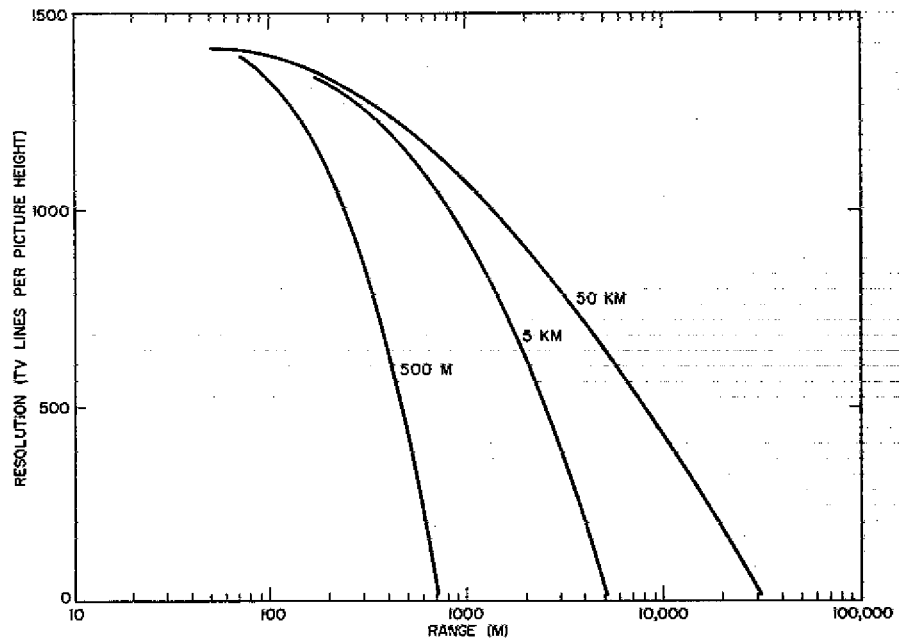


Fig. 11 - Display resolution vs range for the system of Fig. 3 with two image intensifiers added

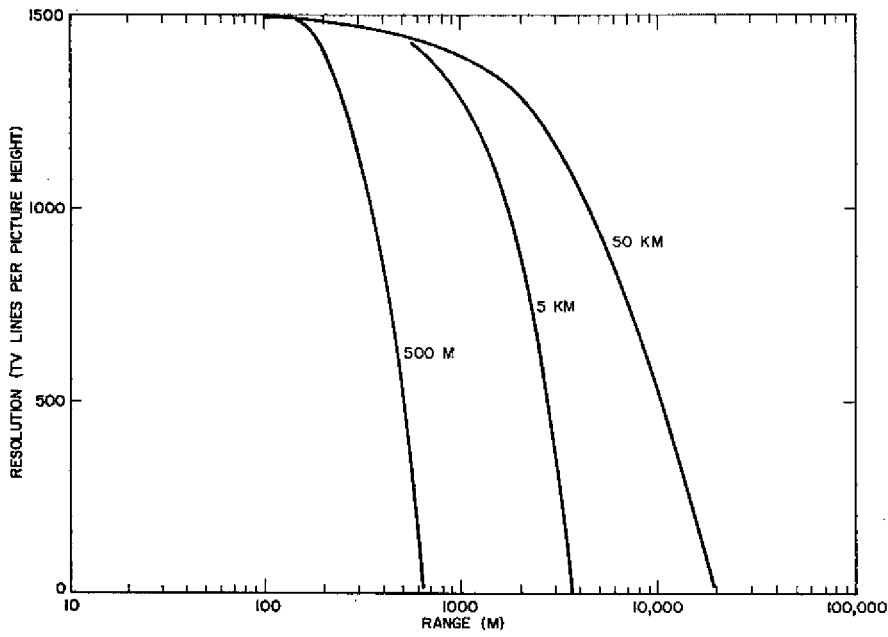


Fig. 12 - Display resolution vs range for the system of Fig. 4 with one image intensifier added

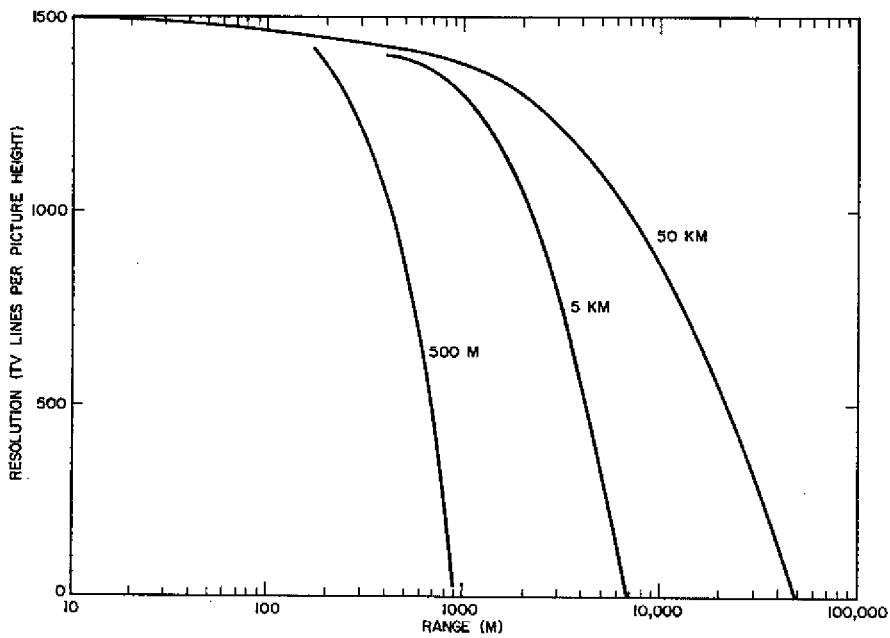


Fig. 13 - Display resolution vs range for the system of Fig. 4 with two image intensifiers added

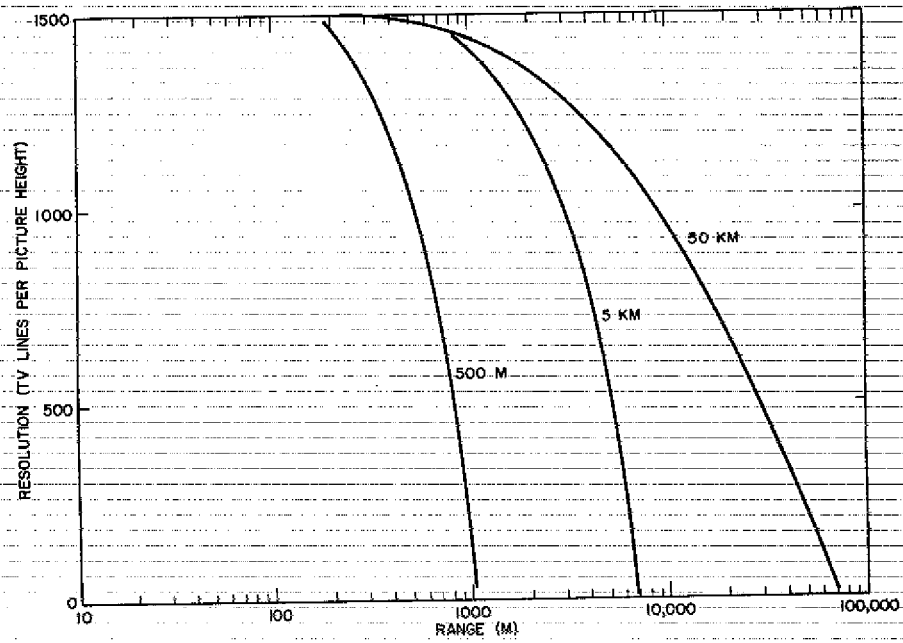


Fig. 14 - Display resolution vs range for the system of Fig. 5 with one image intensifier added

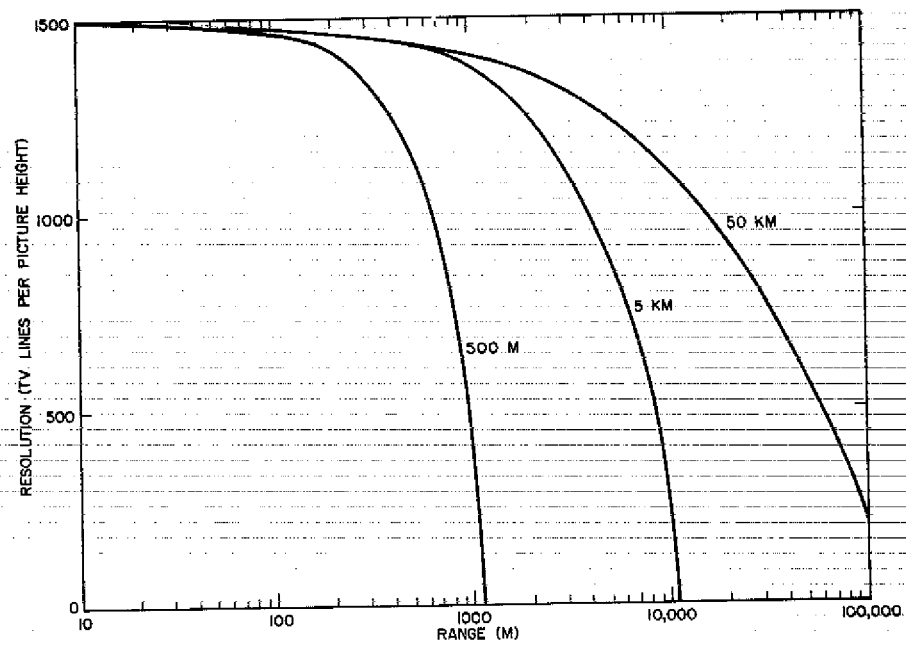


Fig. 15 - Display resolution vs range for the system of Fig. 5 with two image intensifiers added

## UNDERWATER APPLICATIONS

The undersea environment is another place where an active imaging system may have application. Deep-ocean search operations could be aided in much the same way as airborne reconnaissance. The ability of the ocean to transmit light is extremely poor. Nevertheless, an laser-scanned active imaging system mounted in a deep-submergence vehicle or in a towed "fish" would offer both real-time viewing capabilities and improved range or resolution. The applicability of the scanned system to the underwater environment can be presented in a manner similar to the analysis previously given.

### Light Transmission in the Sea

In the sea, both absorption and scattering play important roles. Both of these effects can be lumped together by the attenuation coefficient  $\alpha$  ( $\text{m}^{-1}$ ). Considerable effort has been made to study the propagation of light in sea water (3-6). Harford (7) summarizes the available data. Maximum transmission occurs at wavelengths between 4500 Å and 5500 Å. The attenuation coefficient varies greatly, ranging from 0.18 to 0.35  $\text{m}^{-1}$  for coastal water and from 0.04 to 0.15  $\text{m}^{-1}$  for ocean water. No information is available as a function of depth, but values for pure water are about 0.01  $\text{m}^{-1}$ .

On the basis of wavelength and power, two lasers may be useful for illumination. The argon laser can provide as much as 5 W of radiation in the wavelength region of interest. The Nd:YAG laser also runs continuously at power levels of 1 kW or more. Unfortunately, its output wavelength, 10,600 Å, must be frequency doubled to reach a wavelength of 5300 Å. The doubling process at present may reduce the power to 500 W or less.

### Analysis

Characteristics of both laser sources mentioned in the previous section have been used in the theoretical analysis. Attenuation coefficients of 0.1 and 0.01  $\text{m}^{-1}$  have been used, characteristic of ocean water and pure water respectively. Figure 16 shows observer resolution vs range for both 5 W and 500 W power and for an attenuation coefficient of 0.01  $\text{m}^{-1}$ . It should be noted that a hundredfold increase in power does not double the range of a specific resolution — a vivid example of the severity of sea water on optical transmission. Figure 17 shows the effects of reduced contrast on resolution for the 500-W system for which  $\alpha = 0.01 \text{ m}^{-1}$ .

These systems seem to offer advantages over present methods of deep-ocean search. Present techniques use photographic equipment and strobe lights mounted on a towed "fish" to record pictures when other sensing devices indicate objects are present. The fish must be towed at distances of only about 5 m from the ocean floor — a difficult task at 2500-m depths. Also, the fish must be retrieved and the photographs processed before object detection can be confirmed. The 5-W ( $\alpha = 0.01 \text{ m}^{-1}$ ) system has a 500-TV-lines-per-picture-height resolution at 250 m from the bottom and provides real-time information. At this distance, with a lens of 1-ft focal length, the observer should be able to recognize an object about 1 ft in size. Permanent records of the video display could be made via video tape or film.

It is interesting to consider whether image intensifiers might aid the system in the underwater environment. The analysis is identical to the atmospheric cases. Figure 18 shows the effects of one and two intensifiers with the 5-W ( $\alpha = 0.01 \text{ m}^{-1}$ ) system. At short distances the poorer aperture response degrades the resolution. At longer distances some improvement is noted, but is slight and perhaps not worth the effort.

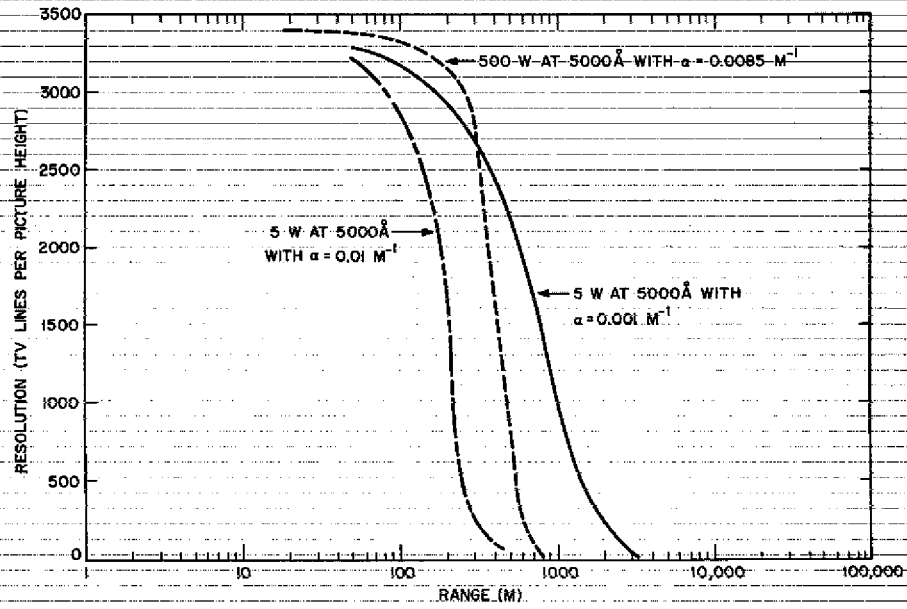


Fig. 16 - Display resolution vs range for a 5000-Å laser emitting 5 W in sea water with  $\alpha = 0.01 \text{ m}^{-1}$  and  $0.001 \text{ m}^{-1}$  and 500 W in sea water with  $\alpha = 0.0085 \text{ m}^{-1}$  (100% contrast)

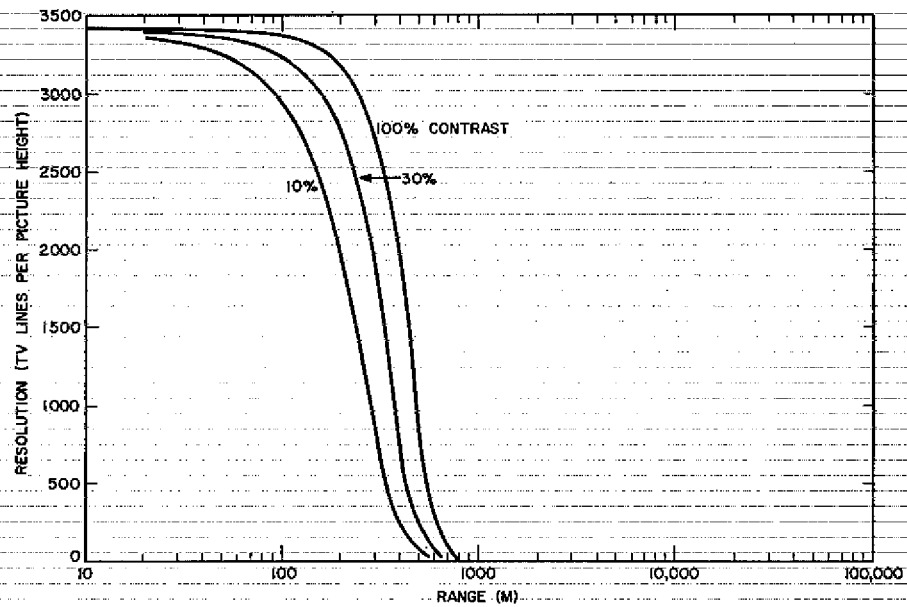


Fig. 17 - Display resolution vs range for a 5000-Å, 500-W laser in sea water with  $\alpha = 0.0085 \text{ m}^{-1}$  and for 100%, 30%, and 10% contrast

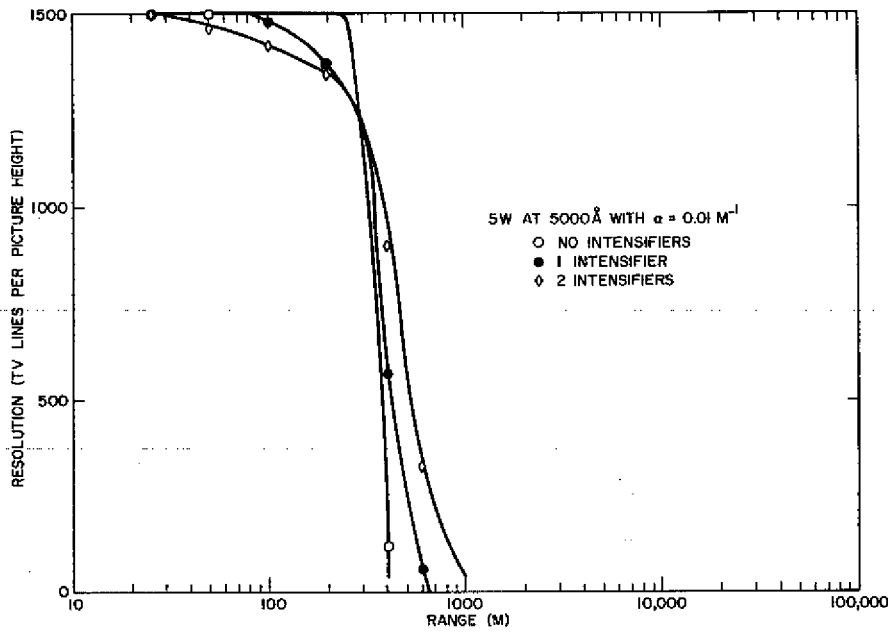


Fig. 18 - Display resolution vs range for the 5-W, 5000-Å system operating in water with  $\alpha = 0.01 \text{ m}^{-1}$  with no intensifier, one intensifier, and two intensifiers. (The system with no intensifiers would actually approach 3400 TV lines/picture-height resolution, but the curve is terminated here for plotting ease.)

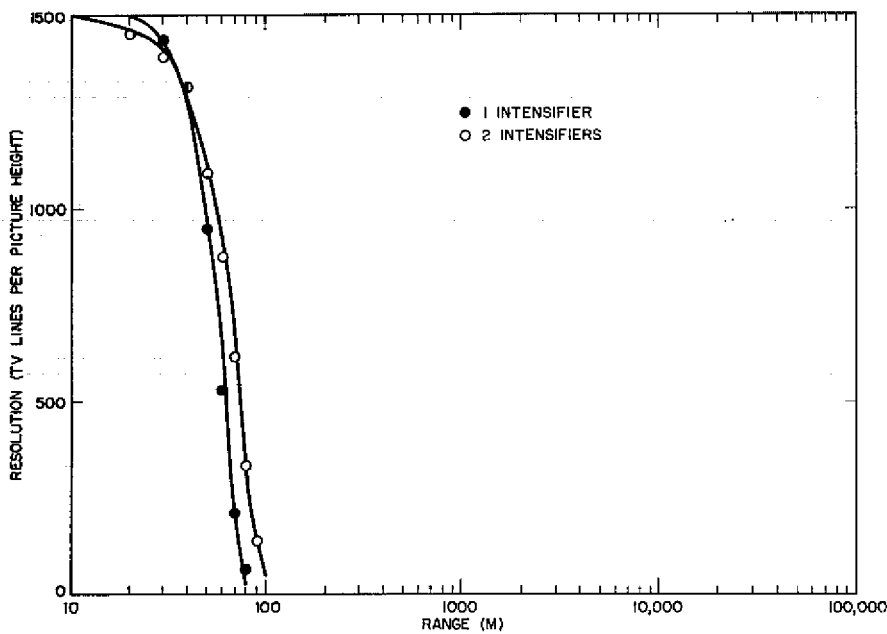


Fig. 19 - Display resolution vs range for the 5-W, 5000-Å system in severely attenuating sea water ( $\alpha = 0.1 \text{ m}^{-1}$ ) with one and two image intensifiers. This system could produce a real-time display with commercial-TV resolution (500 TV lines) of the sea bottom while "floating" 75 m above the sea bottom in an extremely severe sea environment.

Figure 19 shows the results when  $\alpha = 0.1 \text{ m}^{-1}$ . Here even two intensifiers cannot bring 500-TV-line resolution beyond about 70 m.

#### SUMMARY

The scanned-laser active imaging system shows considerable promise as an alternative to the gated system. With presently available laser sources, reasonable resolution at respectable ranges can be obtained in the atmosphere. The system is also applicable to the underwater environment and offers the advantages of improved range and real-time viewing which are not presently available.

The theoretical analysis is only a prediction of how well an observer would perform, but based on the success of Rosell (1), it should be accurate. Hopefully the results will stimulate an attack on the practical problems associated with the realization of the system.

#### ACKNOWLEDGMENT

The author is indebted to Mr. Fredrick A. Rosell for helpful discussions during the initial work at Westinghouse.

#### REFERENCES

1. Steingold, H., and Strauch, R.E., Appl. Opt. 8, 147 (1969)
2. Rosell, F.A., J. Opt. Soc. Am. 59, 539 (1969)
3. Lankes, L.R., Opt. Spectra 4, No. 5, 42 (1970)
4. Duntley, S.Q., Opt. Spectra 1, 64 (1967)
5. Duntley, S.Q., J. Opt. Soc. Am. 53, 214 (1963)
6. Heckman, P., Jr., and Hodgson, R.T., IEEE J. Quantum Elec. 3, 445 (1967)
7. Harford, J.W., "Underwater Light and Instrumentation" in Handbook of Ocean and Underwater Engineering (John J. Myers, Carl H. Holm and Raymond F. McAllister, editors), McGraw-Hill, N.Y., 1969, pp. 3-24